Hybrid MHD/PIC simulation of a metallic gas-puff z pinch implosion

IOP Conf. Series: Journal of Physics: Conf. Series **1115** (2018) 022014 doi:10.1088/1742-6596/1115/2/022014

Hybrid MHD/PIC simulation of a metallic gas-puff z pinch implosion

D L Shmelev[1,2], V I Oreshkin[3,4] and S A Chaikovsky[1]

[1]Institute of Electrophysics, UB RAS, 106 Amundsen Str., Ekaterinburg, 620016, Russia
[2]Ural Federal University, 19 Mira Str., Ekaterinburg, 620002, Russian
[3]Institute of High Current Electronics SB RAS, 2/3 Akademichesky Ave., Tomsk, 634055, Russia
[4]National Research Tomsk Polytechnic University, 30 Lenin Ave., Tomsk, 634050, Russia

E-mail: shmelev@iep.uran.ru

Abstract. We present the hybrid MHD/PIC simulations of the time evolution of a bismuth metallic gas-puff z pinch in external axial magnetic field (AMF). Recent experiments with IMRI-5 generator (450 kA, 450 ns) [1] show the certain effect of an axial magnetic field on radiation energy produced during z pinch implosion. In order to perform the numerical simulation of gas puff z pinch a hybrid model was developed. The hybrid model treats the electrons as a massless fluid and ions as macroparticles. The macroparticle dynamic is calculated with the use of PIC method. Ion-ion Coulomb collision is considered with the use of MC method. The radiation transfer of bismuth plasma was accounted in the framework of P1 method. The interelectrode gap pumping by plasma of 8 μs 80 kA bismuth arc with the following plasma implosion by 450 kA/ 450 ns current pulse in different external AMF was modelled. The obtained results are in a reasonable agreement with the experimental results.

1. Introduction

The metallic gas-puff z-pinch are formed by injecting high-current vacuum arc plasma into a vacuum gap the electrodes of which are under the voltage supplied by a generator to produce the z pinch. A number of studies [1-3] show that the plasma liners thus generated have a smoothly decreasing with an increase of radius density profile (so called tailored profile). According to [4], the liner with density profile subject to power law of density reduction suppresses the development of Rayleigh–Taylor instability during the implosion of the z-pinch that results in more homogeneous compression involving almost all substance of the liner. In case of compression of a sharp boundary liner, the Rayleigh–Taylor instabilities develop in the current sheath that makes only a part of the liner substance to compress [5]. As some experimental researches [1-2] reveal, the liner formed by injecting the high current arc plasma compresses homogeneously without any visible disturbances typical for the developed Rayleigh-Taylor instability.

It was shown [1] that energy radiated from the z-pinch can be considerably changed with the help of external AMF the induction of which is much less than the induction of the z-pinch self-magnetic field. Moreover, the total radiated energy of the bismuth plasma z-pinch compressed by IMRI-5

generator (450 kA, 450 ns) non-monotonously depends on external AMF. Initially, when AMF increases from 0 to 3 kGs the radiation energy rises from ~1.5 to ~2.8 kJ. With the further increase in AMF the radiation monotonically decreases. This work is devoted to study of impact of external AMF on the z-pinch dynamics by numerical simulation under configuration (figure 1) similar to the one used in [1].

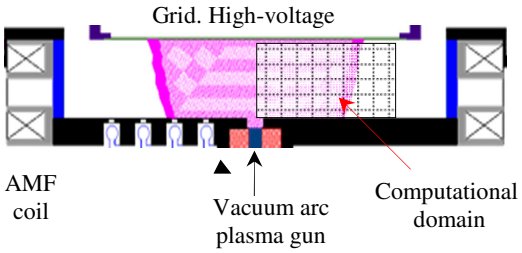

Figure 1. Geometry of the problem.

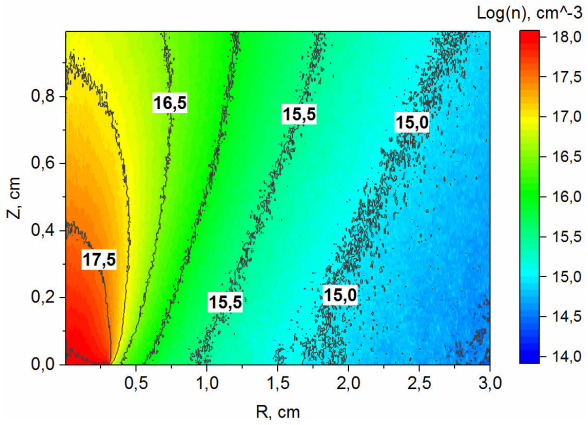

Figure 2. Initial plasma density distribution in computational domain.

2. Model description

The two-dimensional hybrid model of quasi-neutral plasma in the context of 2D axisymmetric geometry developed earlier [6, 7] has been modified into a 2.5-dimensional model. The new modification takes into account the all three components of ion and electron velocities, current and magnetic field, but all the components depend only on the two variables – r and z. This modification of the model allows studying the impact of AMF on plasma liners dynamics.

The developed model is a hybrid one, i.e. ions are treated as the macroparticles with the help of the particles-in-cells (PIC) method (equations (1), (2)). The macroparticles can describe the particles of different type, i.e. the particles having different charge and mass. The electrons are treated as the massless fluid (4), (5). The electromagnetic part in the quasi-neutral approximation is reduced to the equation for the transfer and diffusion of the magnetic field (only θ-component) (6), transfer and diffusion of vector potential θ-component (7) and the equation for the current and the magnetic field (8).

$$\frac{d\vec{r}_i}{dt}=\vec{V}_i;\qquad m_i\frac{d\vec{V}_i}{dt}=e_iE+\frac{e_i}{c}\vec{V}_i\times\vec{B}+\frac{m_en_e}{n_i}\frac{\vec{u}_e-\vec{V}_i}{\tau_{ei}}+\frac{\delta m_i\vec{V}_i}{\delta t}\,, \tag{1}$$

$$n_i=\frac{1}{H_c}\sum_{k=1}^{N_c}S(x-x_k);\quad n_i\vec{u}_i=\frac{1}{H_c}\sum_{k=1}^{N_c}\vec{V}_k\,S(x-x_k);\quad n_iT_i=\frac{2}{3}\frac{1}{H_c}\sum_{k=1}^{N_c}\frac{m_i\left(\vec{V}_k-\vec{u}_i\right)^2}{2}S(x-x_k)\,, \tag{2}$$

$$\vec{E}=-\frac{\vec{\nabla}P_e}{en_e}-\frac{1}{c}\vec{u}_e\times\vec{B}-\frac{m_e}{e}\sum_i\frac{\vec{u}_e-\vec{u}_i}{\tau_{ei}} \tag{3}$$

$$n_e=\frac{1}{e}\sum_i e_in_i;\qquad \vec{u}_e=\frac{1}{en_e}\left(\sum_i e_in_i\vec{u}_i-\vec{J}\right), \tag{4}$$

$$\frac{3}{2}n_e\left(\frac{\partial T_e}{\partial t}+\vec{u}_e\nabla T_e\right)+P_e\vec{\nabla}\cdot\vec{u}_e+\vec{\nabla}\gamma\frac{n_eT_e\tau_{ei}}{m_e}\vec{\nabla}T_e=\frac{\vec{J}^2}{\sigma}-\frac{3m_e}{\tau_{ei}}(T_e-T_i)-W_{rad}-W_{ion} \tag{5}$$

$$\frac{\partial B_\theta}{\partial t}+\frac{\partial u_{ez}B_\theta}{\partial z}+\frac{\partial u_{er}B_\theta}{\partial r}-\frac{\partial u_{e\theta}B_z}{\partial z}-\frac{\partial u_{e\theta}B_r}{\partial r}=\frac{c^2}{4\pi}\left(\frac{\partial}{\partial r}\left(\frac{1}{r\sigma}\frac{\partial rB_\theta}{\partial r}\right)+\frac{\partial}{\partial z}\left(\frac{1}{\sigma}\frac{\partial B_\theta}{\partial z}\right)\right), \quad (6)$$

$$\frac{\partial A}{\partial t}+u_{ez}\frac{\partial A}{\partial z}+\frac{u_{er}}{r}\frac{\partial rA}{\partial r}=\frac{c^2}{4\pi}\frac{1}{\sigma}\left(\frac{\partial}{\partial r}\left(\frac{1}{r}\frac{\partial rA}{\partial r}\right)+\frac{\partial}{\partial z}\left(\frac{\partial A}{\partial z}\right)\right) \quad (7)$$

$$B_z=\frac{1}{r}\frac{\partial rA}{\partial z},\ B_r=-\frac{\partial A}{\partial z},\quad \vec{J}=\frac{c}{4\pi}\nabla\times\vec{B} \quad (8)$$

where V_i – velocity of the ion macroparticle of i-type, r_i – radius vector of i-type macroparticle, S – weighting function of PIC method (the bilinear interpolation is presently used), H_c – volume of PIC cell, N_c – number of particles in cell, n_i – density if i-type ions, n_e – electrons density, u_i – drift velocity of i-type ions, u_e – electrons drift velocity, J – current density, τ_{ei} – electron-ion collision time, σ – plasma conductivity, B – magnetic field, E – electric field (in the context of quasi-neutrality), P_e – electron pressure, W_{rad} – radiation losses, W_{ion} – losses of energy for ionization, A-θ – component of vector potential. The last term in the right part (1) formally indicates the change of macroparticles impulse caused by Coulomb ion-ion collisions. In the approach developed in this work these collisions are modeled with the use of Monte Carlo method (MC) [9].

The losses of energy for ionization in (5) are calculated in the course of modeling of ionization and recombination reactions. The reactions are modeled with the help of direct simulation Monte Carlo method (DSMC) with the use of zero collision technique to speed up the calculations. Direct ionization, triple recombination, photorecombination are taken into account.

The radiation losses W_{rad} in (5) are calculated in course of computation of radiation transfer with the use of P1 method. For this purpose, a preliminary calculation of absorption coefficients k_ν was performed using the truncated hydrogen atom model for each sort of ions [8] with density equal to unity (in units of the computation) and under different temperatures in multiband approximation (six-band in this case). In the course of computation the concentration of each type of ions is estimated, and then multiplied by the coefficient interpolated for a certain temperature, and after summation over all types of ions the absorption coefficient is obtained. Then, the following equation is solved for each band:

$$\nabla\cdot\left(\frac{1}{k_\nu}\nabla G_\nu\right)=3k_\nu\left(G_\nu-4\pi G_{b\nu}\right) \quad (9)$$

where $Gb_{b\nu}$ – Planck function integrated over ν-th frequency range, after that the total radiation losses are calculated

$$W_{rad}=\sum_{\nu=1}^{6}k_\nu\left(G_\nu-4\pi G_{b\nu}\right)\cdot \quad (10)$$

Six spectral bands were used for computation of Bi: band 1 – 0-25 eV; band 2 – 25–57 eV; band 3 – 57-128 eV; band 4 – 128-260 eV; band 5 – 260-515 eV; band 6 – 515-1000 eV.

Compression dynamics is regulated by solving the system of the electric circuit equations with the following circuit parameters: L_0=25 nG, C_0=3,2 μF, initial voltage $U(0)$=40 kV. In the case of the short circuit the circuit provides current $I(t)=I_{max}\sin((\pi/2t_0)t)$, where t_0 is about 450 ns, I_{max} – about 450 kA, which is in compliance with current source characteristics used in the experiment [1, 2].

The plasma liner compression problem was solved in cylindrical geometry on a rectangular grid. The size of the computational domain: radius – 3 cm, height – 1 cm. The computational cells are square: 50 μm×50 μm. As the computational domain is cylindrical, the cells volume increases linearly with the increase in radius. Due to this the macroparticles have different statistical weight that depends on radius of particle injection into the computational domain. When moving to the center the macroparticles split, thus increasing the number of the particles and reducing the chaotic fluctuations

amplitude of the average values. For computation of the Coulomb scattering of the macroparticles having different statistical weights a special procedure precisely keeping the collisions impulse and energy is used.

3. Results and discussions

The dynamics of z pinch compression and the total radiation output are mainly determined by initial spatial distribution of plasma liner density in the interelectrode gap. The initial plasma distribution is estimated by computation of plasma expansion from the cathode sources having configuration close to that of the experiments. There is the central plasma source with 0.3 cm radius. The source injects (figure 1) fully ionized bismuth plasma with the following parameters: ions charge – 2, temperature 2 eV, drift velocity – $5 \cdot 10^5$ cm/s [10], dispersion angle – 90 within 7.5 microseconds. The quantity of plasma in the interelectrode gap and mass of the liner prior to the compression are varied by setting specific erosion of the sources. Preliminary computation has shown that the liner should have the linear mass of ~80 μg/cm to compress within ~450 ns. At that, the specific erosion should be equal to 520 μg/C, that is almost three times as big as the erosion measured for low-current arc on Bi cathode [11]. Calculation of plasma expansion was carried out without external AMF. During further computation of plasma liner compression at different AMF the initial plasma distribution (figure 2) remained unchanged.

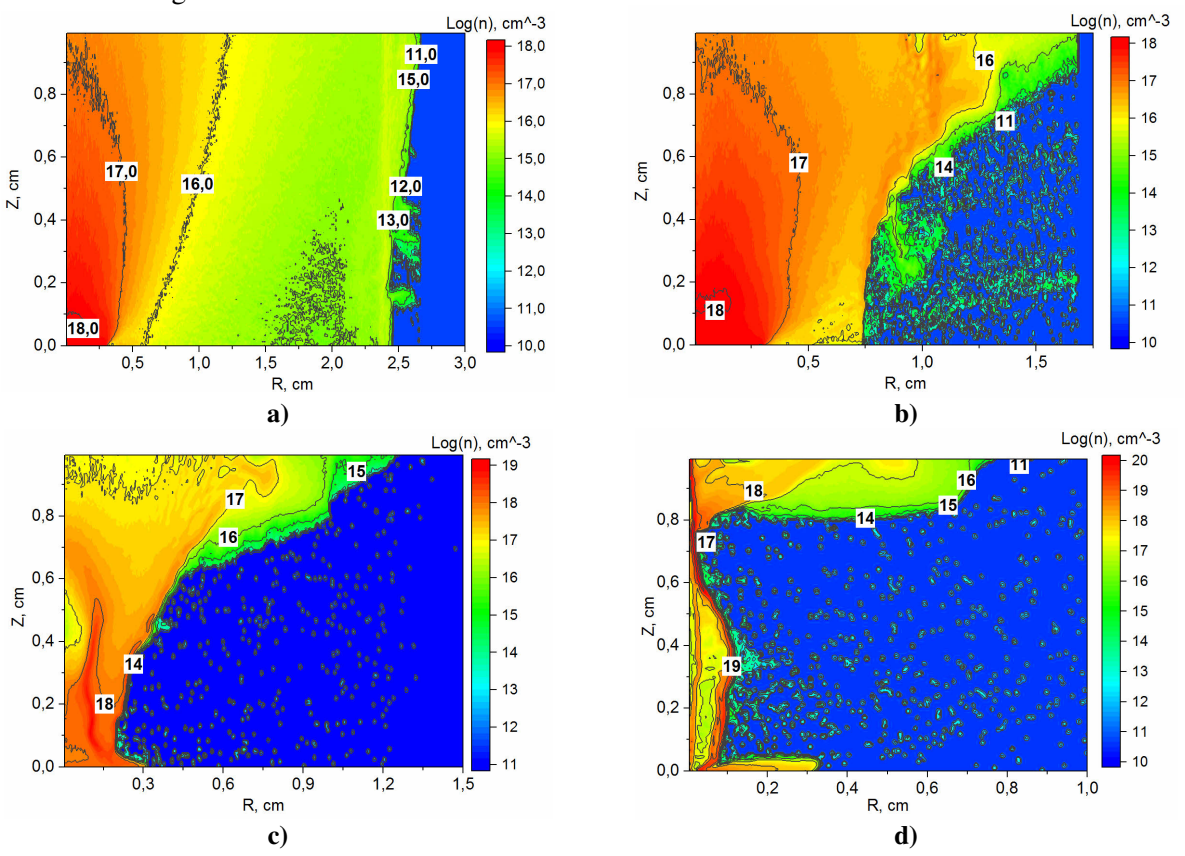

Figure 3. Compression of plasma liner. a) 0.2 μs; b) 0.4 μs; c) 0.46 μs; d) 0.51 μs. AMF – 0.3 T.

In (figure 2) we can see that plasma density distribution along *r* has smoothly decreasing density profile. As it was assumed [4], during current sheath compression the large-scale Rayleigh-Taylor instabilities do not develop and the liner compresses quite homogeneously (figure 3).

The total radiation power (sum over all bands) and current variation are shown in figure 4. It can be seen that in case of AMF – 0.1 T the pinch compresses significantly earlier than it does in case of

larger fields, thus, the pinch current decreases faster. As a result, less energy is injected into the liner and, accordingly, less energy is radiated (figure 5). This is one of the reasons of dependence of the total radiation energy on AMF. Another reason is deceleration of the pinch plasma expansion by external AMF after the first compression. The example of such expansion is represented in figure 3d. The expansion proceeds not so fast as it would in the absence of the field and the pinch radiates longer.

Figure 5 shows that the liner total radiation energy obtained from the calculation is about 1 kJ, that coincides (in terms of the order of magnitude) with the energy generated during the experiment [1].

The obtained energy – AMF dependence is also non-monotonous. It should, however, be mentioned that the energy output considerably depends on the initial plasma distribution which is set by the plasma gun operation mode. Variation of the gun operation modes during the computation has shown that the radiation energy stays at the same level, but the nature of the dependence of the radiation on AMF can change.

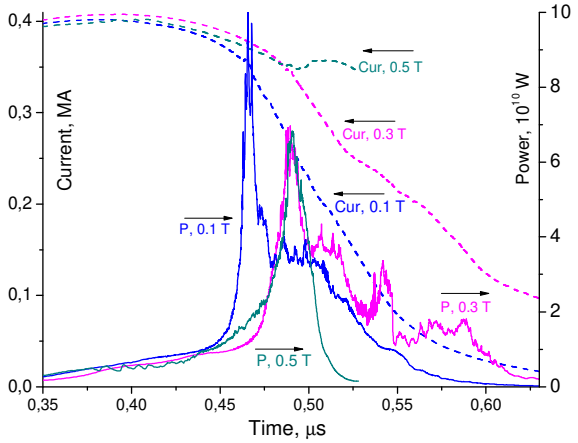

Figure 4. Total radiation power (sum over all bands)-right scale, current (left scale) versus time for different AMF

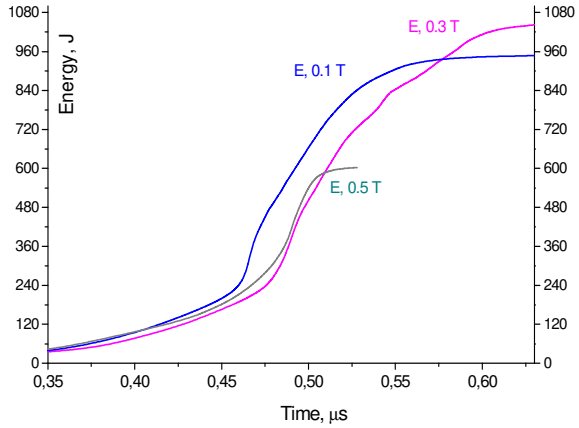

Figure 5. Total radiation energy versus time for different AMF.

Acknowledgments
The work was supported by Russian Science Foundation (project No. 16-19-10142).

References

[1] Rousskikh A G, Zhigalin A S, Oreshkin V I, Frolova V, Velikovich A L, Yushkov G Yu and Baksht R B 2016 *Phys. Plasmas*. **23** 063502
[2] Rousskikh A G, Zhigalin A S, Oreshkin and Baksht R B 2017 *Phys. Plasmas* **24** 063519
[3] Rousskikh A G, Baksht R B, Zhigalin A S, Oreshkin V I, Chaikovsky S A and Labetskaya N. A 2012 *Plasma Phys. Rep.* **38** 595
[4] Velikovich A L, Cochran F L and Davis J 1996 *Phys. Rev. Lett.* **77** 853
[5] Welch D R, Rose D V, Thoma C, et al. 2010 *Phys. Plasmas* **17** 072702
[6] Shmelev D L and Uimanov I V 2015 *IEEE Trans. Plasma Sci*. **43** 2261
[7] Shmelev D L, Oreshkin V I and Chaikovsky S A 2017 *J. Phys.: Conf. Series* **830** 012018
[8] Oreshkin V I 2013 *Radiation of High-Temperature Plasmas: Pinch Effect* (LAP LAMBERT: Academic Publ.)
[9] Bobylev A V and Potapenko I F 2013 *J. Comp. Phys.* **246** 123
[10] Yushkov G Yu, Anders A, Oks E M and Brown I G 2000 *J. Appl. Phys.* **88** 5618
[11] Anders A, Oks E M, Yushkov G Yu, et al. 2005 *IEEE Trans. Plasma Sci.* **33** 1532